Iranian Journal of Fuzzy Systems

Volume 21, Number 6, (2024), pp. 147-171

Original paper

University of Sistan and Baluchestan

Type-II fuzzy inference system-based fractional terminal sliding mode control for zero-force exoskeleton robots

M. Mirzaee [1] and R. Kazemi [2]

[1,2] *Faculty of Mechanical Engineering, K.N. Toosi University of Technology, Tehran, Iran*

mortezamirzaee@email.kntu.ac.ir, kazemi@kntu.ac.ir

Abstract

Upper-limb exoskeleton robots have a significant impact on rehabilitation, assistive technology, and human augmentation, as they can restore or enhance human physical abilities. This paper presents a novel control approach, called Adaptive Fractional Integral Terminal Sliding Mode (AFITSM), which combines an exponential reaching law with a unique interval type-2 Fuzzy Inference System (FIS). This controller is designed to achieve zero-force control of a 5-degree-of-freedom upper-limb exoskeleton robot, even in the presence of bounded uncertainties. The controller's integral terminal sliding surface ensures that the system converges in a finite time, allowing the exoskeleton to reach its desired state quickly, which is critical in time-sensitive applications. The exponential switching control term reduces chattering and tracking errors, while the AFITSM controller's adaptability, enabled by the interval type-2 FIS, allows it to adjust its parameters in real-time to handle uncertainties and external disturbances. Numerical simulations demonstrate the effectiveness and superiority of the proposed control method over traditional control approaches.

Keywords: Zero-force control, adaptive control, fractional sliding mode control, exoskeleton robot, fuzzy inference system.

1 Introduction

Exoskeleton robotic systems are intricately designed to enhance human mobility, thereby amplifying the user's physical prowess and agility. These systems are predominantly manifested in the form of upper-limb exoskeleton robots, which are engineered to counteract muscular debility or neurological afflictions. Force control in upper-limb exoskeleton robots is a vital aspect that ensures a smooth and safe interaction between the human user and the robotic system. It involves the regulation of the forces exerted by the robot on the user's limb, thereby enabling the user to perform tasks with increased strength and precision. The force control system is designed to be responsive and adaptive to the user's movements and intentions, providing assistance when needed while allowing for natural and intuitive control of the limb [2]. Zero force control is a specific type of force control strategy used in upper-limb exoskeleton robots. This strategy aims to minimize the force exerted by the robot on the user's limb, essentially making the robot "transparent" to the user. This is particularly useful in applications where the user needs to move freely without any resistance from the robot, such as during rehabilitation exercises or when learning to use the exoskeleton [31].

The efficacy of an exoskeleton robot in providing assistance to the user is fundamentally anchored on the proficiency of the control system. Consequently, researchers have been channeling their efforts towards the development of advanced and robust control strategies to amplify the performance of these robots in a variety of daily living activities [18]. The formulation of robust and adaptive controllers becomes indispensable when navigating the intricate interactions between system states, nonlinearity, and uncertainties that are inherent in upper-limb exoskeleton robots. Sliding Mode Control (SMC) is a method of nonlinear control that has gained increasing prominence in the realm of upper-limb exoskeleton robots, owing to its robustness and efficacy in counteracting disturbances, uncertainties, and nonlinearities. The

Corresponding Author: M. Mirzaee
Received: July 2024; Revised: December 2024; Accepted: January 2025.
https://doi.org/10.22111/ijfs.2025.49399.8718

operational principle of SMC involves compelling the system trajectories to attain and persist on a sliding surface, where the control law can be meticulously crafted to ensure closed-loop stability and tracking performance [17].

Terminal Sliding Mode Control (TSMC) is a technique that can enhance the rate of convergence of a system by incorporating a sliding mode in the terminal phase of the control action. By implementing this, TSMC can accomplish finite-time convergence, signifying that the system attains a desired state within a predetermined time frame. This is in stark contrast to traditional SMC methods, which do not assure finite-time convergence. Furthermore, TSMC can diminish the steady-state error of the system and render it more resilient to uncertainties and disturbances. Additionally, TSMC has been applied in a wide range of applications, including control of robotic systems, spacecraft, renewable energy systems, and power electronics, due to its robustness and high precision [32]. The fractional-order (FO) integral and differential calculus have garnered significant attention in the realm of TSMC due to their ability to provide a higher degree of freedom in comparison to their integer-order counterparts. This increased flexibility enables the TSMC to exhibit enhanced performance and adaptability in a wide range of applications [21].

The performance of SMC is significantly contingent on its parameters, which can be arduous to determine. Intelligent systems, such as Fuzzy Inference Systems (FISs) and neural networks, can be employed to surmount this challenge by adapting the controller parameters to diverse operating conditions. This results in a more robust and effective control of exoskeletons by enhancing their capacity to manage uncertainties and external disturbances. Adaptive intelligent controllers can further augment the performance of exoskeletons by perpetually adjusting the controller parameters based on feedback from the system. FIS can address these challenges by approximating the uncertain nonlinear functions and optimal gains of controllers. The interval type-2 FIS is devised to more effectively manage the uncertainty of the control system and bolster its robustness. In interval type-2 FIS, all of the crisp membership functions are assumed as an interval, hence the uncertainty can be efficiently managed by the interval membership functions [4].

In this article, the Adaptive Fractional Integral Terminal Sliding Mode (AFITSM) controller, coupled with an exponential reaching law and utilizing an interval type-2 FIS, is introduced for zero-force control of a 5-DOF upper-limb exoskeleton robotic system in the presence of bounded uncertainties.

- **Adaptive Control:** The AFITSM controller is adaptive, meaning that it can adjust its parameters in real-time based on feedback from the system. This renders the controller more robust and flexible, enabling it to handle uncertainties and external disturbances that may impact the performance of the exoskeleton.
- **Novel Type-2 Fuzzy Inference System (T2FIS):** The controller utilizes a novel modified T2FIS, which is specifically designed to handle uncertainty more effectively. The T2FIS can capture and manipulate uncertainties in a more comprehensive and nuanced manner, allowing the controller to make more informed decisions and respond more accurately to changing conditions. This integration of adaptive control and advanced fuzzy logic enables the AFITSM controller to provide exceptional performance and reliability in a wide range of scenarios.
- **Fractional Integral Terminal Sliding Mode:** The AFITSM controller employs Fractional Integral Terminal Sliding Mode (FITSM) surface, which can ensure finite-time convergence of the system. This implies that the exoskeleton can reach its desired state within a specified duration, which can be vital in time-sensitive applications.
- **Chattering Mitigation:** The innovative exponential switching control term effectively reduces the chattering phenomenon, a common issue in sliding mode control systems. Furthermore, the transient and steady-state tracking error is significantly mitigated, resulting in improved overall system performance. Moreover, the incorporation of this control term leads to an increased convergence rate, allowing the system to reach its desired state more rapidly and efficiently.
- **Global Stability:** The AFITSM controller is engineered to ensure the global stability of the system, signifying that it can guarantee stability for any initial condition. This is a crucial consideration in exoskeleton control, where safety and reliability are paramount.

The proposed control method is substantiated by numerical simulations that demonstrate its feasibility and superiority over certain conventional control methods such as conventional SMC and the methods in with adaptive passivity-based [11]. The proposed Adaptive AFITSM controller offers several advantages and benefits for exoskeleton robots, including improved adaptability and robustness, enhanced convergence speed, and effective chattering mitigation. The integration of adaptive control, type-2 fuzzy control, fractional order computation, and terminal sliding mode control enables the AFITSM controller to handle uncertainties and external disturbances, capture complex and nonlinear dynamics, and achieve finite-time convergence. Overall, the AFITSM controller provides improved control performance and stability, making it a suitable solution for exoskeleton robots operating in uncertain and dynamic environments.

The structure of the paper is as follows. Section 2 elucidates the dynamic model of the upper-limb exoskeleton robot and the architecture of the zero-force control. Section 3 delineates the proposed AFITSM controller with the exponential reaching law. The numerical simulations showcased in the paper play a pivotal role in validating the proposed method and underscoring its superiority over existing methodologies. Lastly, the conclusion section encapsulates the results and underscores the importance of the proposed control method in the realm of exoskeleton robotics.

2 System description

In this section, the dynamic model of a 5-DOF upper-limb exoskeleton robot for zero-force controlling is described using Lagrange and state space equations. Equ. (1) represents the Lagrange equation, which relates the position, velocity, and acceleration vectors of the robot to its torque inputs, external forces, and inertia, Coriolis and, and gravity.

$$M(q)\ddot{q} + C(q,\dot{q})\dot{q} + G(q) + f = u, \tag{1}$$

where $q, \dot{q}, \ddot{q} \in \mathbb{R}^5$ represent the position, velocity, and acceleration vectors of the robot, respectively. The terms u and f represent the torque inputs and external forces. $M(q)$, $C(q,\dot{q})$, and $G(q)$ denote the inertia matrix, Coriolis and centripetal matrix, and gravity vector, respectively. The nonlinearity of the system is primarily caused by the dependence of the inertia matrix (M), Coriolis matrix (C), and gravity vector (G) on the joint positions (q) and velocities ($\dot{q}$), involving many nonlinear operators such as sin and cos. This dependence introduces complex interactions between the system's variables, resulting in a highly nonlinear and coupled system dynamics. For a comprehensive description of the system's model, including detailed derivations and formulations, the reader is referred to references [10] and [22].

- **Assumption 1:** All the position, velocity, and acceleration vectors are measurable and have well-defined upper bounds. Moreover, their first and second derivatives with respect to time exist and are also bounded.
- **Assumption 2:** The inertia matrix $M(q)$ is positive definite and symmetric. Additionally, it has a well-defined upper bound.
- **Assumption 3:** The input force vector f is bounded by a constant n, such that $\|f\| \leq n$, where n is chosen to ensure the stability and accuracy of the control system.
- **Assumption 4:** Sensor measurements are assumed to be accurate, noise-free, and free from uncertainty.
- **Assumption 5:** Actuators have instantaneous speed response, no delay or lag, unlimited capacity, and are not subject to saturation.

2.1 Zero-force control

Zero-force control is a type of control strategy used in robotics and automation systems to achieve a desired force or torque at the end effector (e.g., gripper or tool) of a robot. This is in contrast to position control, where the goal is to achieve a specific position or trajectory. Zero-force control can be useful in applications where it is important to maintain a consistent force or torque, such as in assembly operations or when handling fragile objects. The Denavit-Hartenberg parameters are needed for zero-force controlling and it is the represented in [8]. The transfer matrix from the origin in the fixed member to the hand can be obtained from the following equation.

$$T = T_0^1 \times T_1^2 \times T_2^3 \times T_3^4 \times T_4^5, \tag{2}$$

where the matrix of transformations between both members is calculated as follows Denavit-Hartenberg parameters as

$$T_0^1 = \begin{bmatrix} \cos(q_0) & 0 & \sin(q_0) & 60.35\sin(q_0) \\ \sin(q_0) & 0 & -\cos(q_0) & 60.35\cos(q_0) \\ 0 & 1 & 0 & 0 \\ 0 & 0 & 0 & 1 \end{bmatrix}. \tag{3}$$

$$T_1^2 = \begin{bmatrix} \cos(q_1) & -\sin(q_1) & 0 & \text{scap}\cos(q_1) \\ \sin(q_1) & \cos(q_1) & 0 & \text{scap}\sin(q_1) \\ 0 & 0 & 1 & 0 \\ 0 & 0 & 0 & 1 \end{bmatrix}. \tag{4}$$

$$T_2^3 = \begin{bmatrix} \sin(q_2) & 0 & \cos(q_2) & \text{link}\cos(q_2) \\ -\cos(q_2) & 0 & \sin(q_2) & \text{link}\sin(q_2) \\ 0 & -1 & 0 & 0 \\ 0 & 0 & 0 & 1 \end{bmatrix}. \tag{5}$$

$$T_3^4 = \begin{bmatrix} 0 & -\sin(q_3) & -\cos(q_3) & -\cos(q_3) \\ 0 & \cos(q_3) & -\sin(q_3) & -\sin(q_3) \\ 1 & 0 & 0 & 0 \\ 0 & 0 & 0 & 1 \end{bmatrix}. \tag{6}$$

$$T_4^5 = \begin{bmatrix} \cos(q_4) & -\sin(q_4) & 0 & 0 \\ \sin(q_4) & \cos(q_4) & 0 & 0 \\ 0 & 0 & 1 & -\text{fullarm} \\ 0 & 0 & 0 & 1 \end{bmatrix}. \tag{7}$$

using the transformation matrices in (4-7), it is easy to obtain the motion of each joint for each motion in the final actuator. By extracting the first three rows from the last column of the matrix, we can get the vector that is actually the position of the final executive, which is represented by x_e. To obtain the Jacobian matrix, we have:

$$\dot{x}_e = J\dot{q}. \tag{8}$$

Now, by using the resulting Jacobian matrix in (9), it is possible to obtain the resulting torque in each joint caused by the force on the final conductor:

$$f = J^T f_e. \tag{9}$$

Where f_e is the three-dimensional force, and f is the force input to the Zero-force control.

2.2 Literature review

SMC is a robust control technique that utilizes a sliding mode to drive the system's state to a desired trajectory, characterized by its ability to achieve finite-time convergence and enhance the system's resilience to uncertainties and disturbances. SMC boasts several advantages over alternative control methods, including its simplicity, robustness, and swift response, which render it a compelling choice for the zero-force control of upper-limb exoskeleton robots [16]. The paper [21] compares sliding mode control and feedback linearization control for upper limb exoskeletons. The implementation of the sliding mode controller assumes a complete measurement of the biological system's dynamics, while the feedback linearization method does not require any information from the biological system. This paper [1] proposes a non-linear active disturbance rejection control method for an upper limb rehabilitation exoskeleton. The method consists of an extended state observer and a non-linear feedback controller. [24] Runners with plantar heel pain exhibit altered foot kinematics during running gait, characterized by increased heel strike angle, reduced ankle dorsiflexion, and excessive foot pronation, which can contribute to the development and maintenance of pain. This study [30] proposes a novel adaptive-intelligent controller for quadcopters based on brain emotional learning (BEL), which mimics the emotional processing of the human brain to improve stability and robustness in uncertain environments. [8] and [23] papers present the design and development of humanoid robots, Baset and RoboMan, with a focus on mechanical design, control systems, and balance control. The papers demonstrate significant contributions to the field of humanoid robotics, showcasing the authors' expertise in designing and developing advanced humanoid robots for research and competition purposes. [33] presents a novel algebraic transformation approach to achieve consensus in multi-agent singular systems, providing a new framework for solving the consensus problem in such systems.

Despite the numerous advantages of SMC, such as resilience and efficacy in coping with disturbances, uncertainties, and nonlinearities, it can suffer from a chattering effect in the control input. This effect induces unwanted high-frequency oscillations of the system, which can pose challenges in the execution of the control scheme. An exponential reaching law works by adjusting the reaching speed of the system trajectories to the sliding surface according to the distance between them [5]. This way, the system can reach the sliding surface quickly when far from it, and slow down when close to it, avoiding excessive switching and chattering. This paper [6] proposes a model-free super-twisting terminal sliding mode controller for trajectory tracking of an n-DOF upper-limb rehabilitation exoskeleton with backlash hysteresis. [34] presents an adaptive fuzzy sliding mode control approach for underwater manipulators, which

effectively suppresses chattering and estimates hydrodynamic disturbances, ensuring improved stability and robustness in underwater manipulation tasks. An advanced observer-based sliding mode control is proposed for lower extremity exoskeleton systems, which harmonizes the movements of the human and the exoskeleton [19]. An adaptive integral sliding mode control is introduced for upper limb rehabilitation exoskeletons, demonstrating robust performance against parameter uncertainties and disturbances [27]. A fast terminal second-order sliding mode control, based on feedback linearization, is proposed to mitigate chattering and enhance convergence for robotic manipulators [9]. This paper [20] proposes an event-triggered SMC mechanism to achieve exponential consensus in fractional-order descriptor nonlinear multi-agent systems.

The intelligent adaptive SMC is a sophisticated control technique that leverages advanced methodologies such as neural networks, fuzzy logic, and adaptive mechanisms to dynamically adjust to uncertainties and disturbances, thereby enhancing the system's stability, robustness, and tracking performance in complex and nonlinear environments. [25] provides a comprehensive survey of fuzzy control systems and their applications in mechatronics, covering theoretical foundations, design methodologies, and practical applications, making it a valuable resource for researchers and practitioners in the field. [29] proposes a hybrid data-driven active disturbance rejection sliding mode control (HDRSMC) approach for tower crane systems, which combines the advantages of data-driven and model-based control methods to achieve improved stability and robustness. The proposed HDRSMC approach is validated through experiments on a tower crane system, demonstrating its effectiveness in rejecting disturbances and achieving precise control. [28] proposes an adaptive integral sliding-mode control strategy for data-driven cyber-physical systems to counteract a class of actuator attacks, ensuring system stability and security. [7] presents a second-order intelligent proportional-integral fuzzy control strategy for twin rotor aerodynamic systems, which combines the advantages of fuzzy logic and traditional control methods to achieve improved stability and robustness. [26] proposes a shortest path planning and efficient fuzzy logic control approach for mobile robots navigating in indoor static and dynamic environments, ensuring safe and efficient movement. The proposed approach combines graph-based path planning with fuzzy logic control to adapt to changing environments and avoid obstacles. [13] presents a comprehensive overview of iterative feedback tuning (IFT) in fuzzy control systems, providing a theoretical framework and practical applications for optimizing fuzzy controller performance. The proposed IFT approach enables the automatic tuning of fuzzy controller parameters to achieve improved control performance and robustness.

3 Controller description

This section presents the FO calculus, the equations for the FITSM controller, interval type II FIS, and the proposed fuzzy AFITSM controller that are essential for the paper, as they help to explain the mathematical foundation of the proposed controller.

3.1 Fractional-order calculus

In this particular subsection, we present several beneficial definitions and observations that aid in comprehending the tactics of the suggested controllers.

Definition 3.1. *The Riemann–Liouville (RL) fractional-order integral is given by:*

$$({}_a^{RL})I_t^q = \frac{1}{\Gamma(q)} \int_a^t (t-\tau)^{q-1} f(\tau)\, d\tau, \quad t > 0, \quad q \in \mathbb{R}^+, \quad \tau \in \mathbb{R}^+. \tag{10}$$

Here, q represents the order of integration, and $\Gamma(\cdot)$ denotes Euler's Gamma function.

Definition 3.2. *The Caputo fractional-order derivative is defined as:*

$$({}_a^{C})D_t^q f(t) = \frac{1}{\Gamma(n-q)} \int_a^t (t-\tau)^{n-q-1} f^{(n)}(\tau)\, d\tau, \quad \alpha \in \mathbb{N}, \quad n \in \mathbb{N}, \quad \tau \in \mathbb{R}^+. \tag{11}$$

Definition 3.3. *The fractional-order operator, based on Definitions 1 and 2, is expressed as:*

$$D^q[f(t)], \quad -1 \leq q \leq 1. \tag{12}$$

Remark 3.4. *The combination of integral-order and fractional-order derivatives is represented as:*

$$\frac{d^n}{dt^n}({}_a^C D_t^q f(t)) = {}_a^C D_t^q \left(\frac{d^n f(t)}{dt^n}\right) = {}_a^C D_t^{q+n} f(t). \tag{13}$$

Remark 3.5. *The fractional-order derivative for the sign function is computed as:*

$$D^q[sign(f(t))] = \begin{cases} > 0, & if\ f(t) > 0, \quad when\ t > 0 \\ < 0, & if\ f(t) < 0, \quad when\ t > 0 \end{cases} \tag{14}$$

The Oustaloup approximation is a widely used method for approximating fractional order derivatives and integrals in control systems. This approximation technique is based on the idea of replacing the fractional order operator with a rational function, which can be easily implemented using integer order transfer functions. The Oustaloup approximation is particularly useful for designing and analyzing fractional order control systems, as it allows for the approximation of fractional order derivatives and integrals using a finite number of poles and zeros. This approximation technique has been widely used in various fields, including control systems, signal processing, and robotics, due to its simplicity and effectiveness in approximating fractional order operators.

In this paper, the Oustaloup approximation method is employed to approximate fractional order integral and derivative operators using an integer order filter of a specified order N within a defined frequency range $[\omega_L, \omega_H]$, effectively enabling the implementation of fractional order control systems.

$$G_f(s) = s^\mu = K \prod_{k=-N}^{N} \frac{s + \omega'_k}{s + \omega_k}, \quad -2 \le \mu \le 2, \tag{15}$$

where ω'_k is the poles, ω_k is the zeros, and K is the gain of the filter. The three parameters ω'_k, ω_k, and K are obtained from the following equations:

$$\omega'_k = \omega_b \left(\frac{\omega_h}{\omega_b}\right)^{\frac{k+N+0.5(1-\mu)}{2N+1}} \tag{16}$$

$$\omega_k = \omega_b \left(\frac{\omega_h}{\omega_b}\right)^{\frac{k+N+0.5(1+\mu)}{2N+1}} \tag{17}$$

$$K = \omega_h^\mu \tag{18}$$

The frequency range for the Oustaloup approximation is a critical parameter that must be carefully selected to match the operating frequency of the system. In this study, the approximation is performed with $N = 10$ and a frequency range of $[0.001, 1000]$ rad/s, which is chosen to accurately capture the system's behavior.

3.2 Fractional-order terminal sliding mode controller

The following equations define the desired output and tracking error for the system. The desired output is defined as a state vector, denoted by

$$e = f_d - f, \quad e = \begin{bmatrix} e_1 & e_2 & e_3 & e_4 & e_5 \end{bmatrix}^T, \tag{19}$$

where e is the force tracking error, and f_d is a zero vector because the desired force control is zero. To apply zero-force control, the dynamic equation of the robot in (1) is transformed into:

$$M(\tilde{q})\ddot{\tilde{q}} + C(\tilde{q}, \dot{\tilde{q}})\dot{\tilde{q}} + G(\tilde{q}) = u - e, \tag{20}$$

For simplicity, we use the following notation:

$$G(\tilde{q}, \dot{\tilde{q}}, \ddot{\tilde{q}}) = M(\tilde{q})\ddot{\tilde{q}} + C(\tilde{q}, \dot{\tilde{q}})\dot{\tilde{q}} + G(\tilde{q}), \tag{21}$$

The conventional integral sliding surface for this system is defined as follows:

$$s = e + \alpha_1 \int_0^T e\, dt, \quad \alpha_1 > 0, \tag{22}$$

The proposed terminal integral sliding surface is suggested in:

$$s = e + \alpha_1 \int_0^T e\, dt + \alpha_2 \int_0^T |e|^\gamma \operatorname{sign}(e)\, dt, \quad \alpha_2, \alpha_1 > 0,\ 0 < \gamma < 2. \tag{23}$$

Remark 3.6. *The proposed terminal integral sliding surface can achieve faster convergence than the conventional integral sliding surface.*

Remark 3.7. *The robustness, convergence rate, chattering, and stability of the control system depend critically on three parameters of the proposed terminal integral sliding surface, namely,* $\alpha_1, \alpha_2, \gamma$*:*

$$s = e + \alpha_1 D^{(q_1)}[e] + \alpha_2 D^{(q_2)}[|e|^\gamma\, sign(e)], \quad -1 < q_1, q_2 < 0,\ \alpha_2, \alpha_1 > 0,\ 0 < \gamma < 2. \tag{24}$$

Remark 3.8. *The fractional-order terminal integral sliding surface (24) can potentially offer improved robustness and stability compared to the traditional terminal integral sliding surface (23), especially in systems with nonlinear and uncertain dynamics.*

Remark 3.9. *One of the significant advantages of the fractional-order terminal integral sliding surface (25) is that it can resolve the non-singularity problem inherent in traditional TSMC methods, which can lead to chattering and instability issues. The use of fractional-order operators can help to mitigate these problems, resulting in a more robust and stable control system.*

With taking the derivative of the proposed terminal integral sliding surface, we have

$$\dot{s} = \dot{e} + \alpha_1 D^{(q_1+1)}[e] + \alpha_2 D^{(q_2+1)}[|e|^\gamma \operatorname{sign}(e)]. \tag{25}$$

The control input consists of two components: the equivalent term u_{eq} and the switching term u_{sw}. The equivalent term is designed as follows:

$$\dot{s} = \dot{e} + \alpha_1 D^{(q_1+1)}[e] + \alpha_2 D^{(q_2+1)}[|e|^\gamma \operatorname{sign}(e)] = 0. \tag{26}$$

According to (17)-(22), we obtain:

$$\dot{G}(q, \dot{q}, \ddot{q}) - \dot{u}_{eq} + \alpha_1 D^{(q_1+1)}[e] + \alpha_2 D^{(q_2+1)}[|e|^\gamma \operatorname{sign}(e)] = 0. \tag{27}$$

The equivalent control term u_{eq} is obtained as follows:

$$\dot{u}_{eq} = \dot{G}(q, \dot{q}, \ddot{q}) + \alpha_1 D^{(q_1+1)}[e] + \alpha_2 D^{(q_2+1)}[|e|^\gamma \operatorname{sign}(e)]. \tag{28}$$

$$u_{eq} = G(q, \dot{q}, \ddot{q}) + \alpha_1 D^{(q_1)}[e] + \alpha_2 D^{(q_2)}[|e|^\gamma \operatorname{sign}(e)]. \tag{29}$$

The control input of the proposed ITSM controller comprises two terms of u_{eq} and u_{sw}; thus, it is expressed as follows:

$$u = u_{eq} + u_{sw}. \tag{30}$$

To enhance the convergence speed and diminish the chattering effect, the novel exponential switching term (reaching law) is devised as follows:

$$u_{sw} = K_1 \operatorname{sign}(s) + K_2 |s|^{0.5} \operatorname{sign}(s) + (K_3 |s| - 1)\,. \tag{31}$$

The ultimate control input is derived as follows:

$$u = G(q, \dot{q}, \ddot{q}) + \alpha_1 D^{(q_1)}[e] + \alpha_2 D^{(q_2)}[|e|^\gamma \operatorname{sign}(e)] + K_1 \operatorname{sign}(s) + K_2 |s|^{0.5} \operatorname{sign}(s) + (K_3 |s| - 1)\,. \tag{32}$$

Remark 3.10. *When the sliding surface vector* $|s|$ *is large, meaning the tracking system states are far from the desired trajectory, the term* $(K_3|s| - 1)$ *becomes important in the reaching phase and can slow down the convergence. However, when the system states are close to or on the sliding surface, the term* $(K_3|s| - 1)$ *becomes negligible and does not affect the control output. This can help lower or avoid chattering, which is a common problem with sliding mode control methods.*

Theorem 3.11 is presented to demonstrate the Lyapunov stability of the system under the proposed FITSM controller.

Theorem 3.11. *The dynamic system (1) fulfills assumptions (1-3) and is regulated using the proposed control input (33). Then, the tracking error of the system will converge to zero in a predetermined time interval, and the closed-loop stability of the system using the FITSM controller is ensured.*

Proof. Equation (30) expresses a Lyapunov candidate function that represents the system's tracking error as follows:

$$V_1 = \frac{1}{2}s^2. \tag{34}$$

The time derivative of the candidate Lyapunov function is obtained as:

$$\dot{V}_1 = s\dot{s}. \tag{35}$$

Equation (31) can be transformed into the form of equation (26), so that:

$$\dot{V}_1 = s\left(\dot{e} + \alpha_1 D^{q_1}[e] + \alpha_2 D^{q_2}[|e|^{\gamma}\text{sign}(e)]\right). \tag{36}$$

Simplifying equation (36) yields:

$$\dot{V}_1 = -s\left(\left(K_3^{|s|} - 1\right) + K_1\right)\text{sign}(s) + K_2|s|^{0.5}\text{sign}(s). \tag{37}$$

Equation (37) illustrates that the derivative of V_1, denoted as $\dot{V}_1$, is semi-negative definite, signifying that its value is always non-positive. If $s > 0$, then we need to show that the expression inside the parentheses is negative for all $s \neq 0$. This can be done by using the fact that s and $\text{sign}(s)$ have the same sign, and that K_1, K_2, and K_3 are positive constants. Therefore, for all $s \neq 0$, we have:

$$\left(K_3^{|s|} - 1 + K_1\right)\text{sign}(s) + K_2|s|^{0.5}\text{sign}(s) < 0. \tag{38}$$

If $s < 0$, then we need to show that the expression inside the parentheses is positive for all $s \neq 0$. This can be done by using the fact that s and $\text{sign}(s)$ have opposite signs, and that K_1, K_2, and K_3 are positive constants. Therefore, for all $s \neq 0$, we have:

$$\left(K_3^{|s|} - 1 + K_1\right)\text{sign}(s) + K_2|s|^{0.5}\text{sign}(s) > 0. \tag{39}$$

Hence, in both cases, we have shown that $\dot{V}_1$ is negative definite. To continue the proof using LaSalle's Invariance Principle, we need to find the largest invariant set where $\dot{V}_1 = 0$ and show that the only solution in this set is the equilibrium point $s = 0$. From equation (32), it can be seen that $\dot{V}_1 = 0$ if and only if:

$$\left(K_3^{|s|} - 1 + K_1\right)\text{sign}(s) + K_2|s|^{0.5}\text{sign}(s) = 0. \tag{40}$$

This implies that:

$$\left(K_3^{|s|} - 1 + K_1\right) = -K_2|s|^{0.5}. \tag{41}$$

Taking the absolute value of both sides and rearranging, we get:

$$K_3^{|s|} - 1 = -K_2|s|^{0.5} - K_1. \tag{42}$$

Since the left-hand side is non-negative, we must have:

$$-K_2|s|^{0.5} - K_1 \geq 0. \tag{43}$$

or equivalently:

$$|s| \geq \left(\frac{K_1}{K_2}\right)^2. \tag{44}$$

But this contradicts the fact that V_1 is positive definite and radially unbounded, which implies that $|s|$ must be bounded. Therefore, the only possible solution that satisfies $\dot{V}_1 = 0$ is $s = 0$. By LaSalle's Invariance Principle, this means that every solution that starts in a neighborhood of $s = 0$ converges to $s = 0$ as $t \to \infty$. Hence, $s = 0$ is asymptotically stable. This completes the proof. □

3.3 Fractional-order terminal sliding mode controller

A fuzzy inference system (FIS) consists of four elements: a fuzzifier, a rule base, an inference engine, and a defuzzifier. The fuzzifier converts the crisp input values into linguistic variables using the membership functions stored in the rule base [13]. The defuzzifier converts the fuzzy output values into crisp output values.

$$A^j = \prod_{i=1}^{n} \mu_{A_i^j}(x_i), \tag{45}$$

where $\mu_{A_i^j}$ denotes the membership grades of the input variable x_i in the fuzzy set A^j, where i is the input index, and A^j is the product of the membership grades [14].

In an interval type-2 fuzzy inference system (IT2 FIS), each interval type-2 membership function (IT2 MF) in the rule antecedent has a lower and an upper membership function (LMF and UMF, respectively) that define an interval fuzzy rule with their upper and lower bounds.

$$\bar{A}^j = \prod_{i=1}^{n} \bar{\mu}_{A_i^j}(x_i). \tag{46}$$

$$\underline{A}^j = \prod_{i=1}^{n} \underline{\mu}_{A_i^j}(x_i). \tag{47}$$

Let $\bar{\mu}_{A_i^j}$ and $\underline{\mu}_{A_i^j}$ denote the upper and lower membership grades of the input variable x_i in the IT2 FIS set A^j, where i is the input index and A^j is the product of the membership grades [15]. Similarly, let $\bar{A}^j$ and $\underline{A}^j$ denote the product of the upper and lower membership grades, respectively. The normalized vector of $\bar{A}^j$ and $\underline{A}^j$ are given by equations (48) and (49).

$$\zeta_L = \frac{\sum_{i=1}^{M} \left((\bar{A}_i + \underline{A}_i) + \Delta A_i \operatorname{sgn}(\underline{m}_i)\right)}{\sum_{i=1}^{M}(\bar{A}_i + \underline{A}_i) + \sum_{i=1}^{M} (\operatorname{sgn}(\underline{m}_i)\Delta A_i)}, \tag{48}$$

$$\zeta_U = \frac{\sum_{i=1}^{M} \left((\bar{A}_i + \underline{A}_i) + \Delta A_i \operatorname{sgn}(\bar{m}_i)\right)}{\sum_{i=1}^{M}(\bar{A}_i + \underline{A}_i) + \sum_{i=1}^{M} (\operatorname{sgn}(\bar{m}_i)\Delta A_i)}. \tag{49}$$

Let ζ_L and ζ_U denote the normalized vector of $\bar{A}^j$ and $\underline{A}^j$, respectively, where $\bar{A}^j$ and $\underline{A}^j$ are the product of the upper and lower membership grades of the (IT2 FIS) sets. Furthermore, let $\underline{m}_i$, $\bar{m}_i$, and ΔA_i denote the expressions given by:

$$\bar{m}_i = \bar{W}_i - \frac{\sum_{i=1}^{M} \left(\bar{A}_i \bar{W}_i\right)}{\sum_{i=1}^{M} \bar{A}_i}, \tag{50}$$

$$\underline{m}_i = \underline{W}_i - \frac{\sum_{i=1}^{M} \left(\underline{A}_i \underline{W}_i\right)}{\sum_{i=1}^{M} \underline{A}_i}, \tag{51}$$

$$\Delta A_i = \bar{A}_i - \underline{A}_i. \tag{52}$$

Using the center of sets type reduction followed by defuzzification (COS TR + D) method [12], the upper and lower output values of the IT2 FIS based on the Mamdani inference scheme are given by equations (53) and (54), respectively.

$$Y_U = \frac{\sum_{i=1}^{M} \left((\bar{A}_i + \underline{A}_i) + \Delta A_i \operatorname{sgn}(\bar{m}_i)\right) \bar{W}_i}{\sum_{i=1}^{M} \left(\bar{A}_i + \underline{A}_i\right) + \sum_{i=1}^{M} (\operatorname{sgn}(\bar{m}_i)\Delta A_i)}, \tag{53}$$

$$Y_L = \frac{\sum_{i=1}^{M} \left((\bar{A}_i + \underline{A}_i) + \Delta A_i \operatorname{sgn}(\underline{m}_i)\right) \underline{W}_i}{\sum_{i=1}^{M} \left(\bar{A}_i + \underline{A}_i\right) + \sum_{i=1}^{M} (\operatorname{sgn}(\underline{m}_i)\Delta A_i)}. \tag{54}$$

Given equations (48) and (49), we can obtain the final output values of the IT2 FIS based on the Mamdani inference scheme and the center of sets type reduction followed by defuzzification (COS TR + D) method. Let Y_U and Y_L denote the upper and lower output values, respectively, and let $\bar{W}_i$ and $\underline{W}_i$ denote the upper and lower centers of the consequent part membership functions (MFs), respectively, as defined by equations (55) and (56):

$$Y_U = \bar{W}^T \zeta_U, \tag{55}$$

$$Y_L = \underline{W}^T \zeta_L. \tag{56}$$

Finally, the overall output is computed as:

$$Y = 0.5\left(Y_U + Y_L\right), \tag{57}$$

where Y is the output of the proposed IT2 FIS. This approach does not take into account the uncertainty associated with each rule in the rule base. To address this limitation, we propose incorporating uncertainty weights in the defuzzification process. Specifically, we assign an uncertainty weight ω_i to each rule in the rule base, which represents the degree of uncertainty associated with that rule. The uncertainty weights can be learned using a machine learning algorithm, such as a neural network, or can be specified by a domain expert. The modified defuzzification process can be represented as follows:

$$Y_U = \frac{\sum_{i=1}^{M}\left(\omega_i(\bar{A}_i + \underline{A}_i) + \Delta A_i \operatorname{sgn}(\bar{m}_i)\right)\bar{W}_i}{\sum_{i=1}^{M}\left(\omega_i(\bar{A}_i + \underline{A}_i)\right) + \sum_{i=1}^{M}\left(\operatorname{sgn}(\bar{m}_i)\Delta A_i\right)}, \tag{58}$$

$$Y_L = \frac{\sum_{i=1}^{M}\left(\omega_i(\bar{A}_i + \underline{A}_i) + \Delta A_i \operatorname{sgn}(\underline{m}_i)\right)\underline{W}_i}{\sum_{i=1}^{M}\left(\omega_i(\bar{A}_i + \underline{A}_i)\right) + \sum_{i=1}^{M}\left(\operatorname{sgn}(\underline{m}_i)\Delta A_i\right)}. \tag{59}$$

where ω_i is the uncertainty weight associated with the i-th rule. The incorporation of uncertainty weights in the defuzzification process allows the Type II Fuzzy Inference System to take into account the uncertainty associated with each rule, leading to more robust and accurate output values. The advantages of the novelty are presented as follows:

- **Improved Robustness:** The incorporation of uncertainty weights allows the system to handle uncertain or noisy data more effectively, leading to more robust output values.
- **Increased Flexibility:** The uncertainty weights can be learned or specified using different methods, allowing for greater flexibility in the design of the system.
- **Enhanced Interpretability:** The uncertainty weights provide additional insights into the uncertainty associated with each rule, allowing for better understanding and interpretation of the system's output.

3.4 Fractional-order terminal sliding mode controller

This subsection presents the formulation, architecture, and stability analysis of the proposed fuzzy AFITSM controller. The aim of this work is to reduce the chattering effect and enhance the robustness of the controller by adapting the gains of k_1 and k_2 throughout the process. The fuzzy input is the error vector and the fuzzy output is the estimated values of k_1 and k_2, denoted by $\hat{k}_1$ and $\hat{k}_2$, respectively. The estimated values of k_1 and k_2 are given by

$$\hat{k}_1 = \hat{w}_{k_1}^T \zeta_U + \hat{w}_{k_1}^T \zeta_L, \tag{60}$$

$$\hat{k}_2 = \hat{w}_{k_2}^T \zeta_U + \hat{w}_{k_2}^T \zeta_L. \tag{61}$$

Let $\hat{w}_{k_1}, \hat{w}_{k_1}, \hat{w}_{k_2}, \hat{w}_{k_2}$ denote the upper and lower centers of the IT2 FIS consequent part, respectively, for values of the gains of the fuzzy AFITSM controller, i.e., $\hat{k}_1$ and $\hat{k}_2$. The optimal values of upper and lower centers of the IT2 FIS consequent part are shown as follows.

$$(\hat{W}_{k_1}^*, \hat{W}_{k_1}^*) = \arg\min\left[\sup|\hat{k}_1 - k_1^*|\right], \tag{62}$$

$$(\hat{W}_{k_2}^*, \hat{W}_{k_2}^*) = \arg\min\left[\sup|\hat{k}_2 - k_2^*|\right]. \tag{63}$$

where $\hat{W}_{k_1}^*$ and $\hat{W}_{k_1}^*$ are the optimal centers of the consequent part corresponding to k_1 and $\hat{W}_{k_2}^*$ and $\hat{W}_{k_2}^*$ denote the optimal centers of the consequent part for k_2 as the IT2 FIS outputs. The optimal values of k_1 and k_2 are given as follows. The optimal values of k_1 and k_2 can be obtained by solving the following equations.

$$k_1^* = \hat{W}_{k_1}^T \zeta_U + \hat{W}_{k_1}^T \zeta_L, \tag{64}$$

$$k_2^* = \hat{W}_{k_2}^T \zeta_U + \hat{W}_{k_2}^T \zeta_L. \tag{65}$$

The error estimations of the IT2 FIS outputs are obtained in

$$\tilde{k}_1 = \hat{k}_1 - k_1^*, \tag{66}$$

$$\tilde{k}_2 = \hat{k}_2 - k_2^*. \tag{67}$$

Theorem 3.12. *Consider the dynamic system of a 5-DOF upper-limb exoskeleton robot and the assumptions (1-3). The proposed control scheme consists of the AFITSM controller and the IT2 FIS. If the control input is given by the following expression, then the tracking error of the system will asymptotically approach zero, and the closed-loop system stability will be guaranteed in the presence of uncertainties and disturbances.*

$$u = M(\tilde{q})\ddot{\tilde{q}} + C(\tilde{q},\dot{\tilde{q}})\dot{\tilde{q}} + G(\tilde{q}) + \alpha_1 D^{(q_1)}[e] + \alpha_2 D^{(q_2)}[|\mathbf{e}|^{\gamma} sign(\mathbf{e})] + \hat{K}_1 sign(s) + \hat{K}_2|\mathbf{s}|^{0.5} sign(\mathbf{s}) + (K_3|\mathbf{s}| - 1), \quad (68)$$

with the adaptation control rules as (69-72):

$$\dot{\hat{W}}_{k_1} = \frac{\eta}{2}|\mathbf{s}|\zeta_L, \quad (69)$$

$$\dot{\hat{W}}_{k_1} = \frac{\eta}{2}|\mathbf{s}|\zeta_L, \quad (70)$$

$$\dot{\hat{W}}_{k_2} = \frac{\eta}{2}|\mathbf{s}|^{1.5}\zeta_L, \quad (71)$$

$$\dot{\hat{W}}_{k_2} = \frac{\eta}{2}|\mathbf{s}|^{1.5}\zeta_U, \quad (72)$$

where η is the adaptation rate.

Proof. The Lyapunov candidate function for the proposed fuzzy AFITSM controller is considered as:

$$V_2 = \frac{1}{2}s^2 + \frac{1}{\eta}\sum_{i=1}^{2}\hat{W}_{k_i}^T\hat{W}_{k_i} + \frac{1}{\eta}\sum_{i=1}^{2}\hat{W}_{k_i}^T\hat{W}_{k_i}. \quad (73)$$

The time derivative of the candidate Lyapunov function (73) is computed in (74):

$$\dot{V}_2 = s\dot{s} - \frac{2}{\eta}\sum_{i=1}^{2}\hat{W}_{k_i}^T\dot{\hat{W}}_{k_i} - \frac{2}{\eta}\sum_{i=1}^{2}\hat{W}_{k_i}^T\dot{\hat{W}}_{k_i}. \quad (74)$$

Substituting (67) into (74) gives:

$$\dot{V}_2 = s(\hat{K}_1\text{sign}(s) + \hat{K}_2|\mathbf{s}|^{0.5}\text{sign}(\mathbf{s}) + (K_3|\mathbf{s}| - 1)) - \frac{2}{\eta}\sum_{i=1}^{2}\hat{W}_{k_i}^T\dot{\hat{W}}_{k_i} - \frac{2}{\eta}\sum_{i=1}^{2}\hat{W}_{k_i}^T\dot{\hat{W}}_{k_i}. \quad (75)$$

By substituting equations (66-67) into equation (75), we obtain the following result.

$$\dot{V}_2 = s\left(\left(\hat{W}_{k_1}^T\zeta_U + \hat{W}_{k_1}^T\zeta_L\right) = \hat{K}_1\right)\text{sign}(s) + \left(\hat{W}_{k_2}^T\zeta_U + \hat{W}_{k_2}^T\zeta_L\right)|s|^{0.5}\,\text{sign}(s) + (K_3|s| - 1) - \frac{2}{\eta}\sum_{i=1}^{2}\hat{W}_{k_i}^T\dot{\hat{W}}_{k_i} - \frac{2}{\eta}\sum_{i=1}^{2}\hat{W}_{k_i}^T\dot{\hat{W}}_{k_i}. \quad (76)$$

Equation (76) can be decomposed into three terms of $\dot{V}_{2-1}$, $\dot{V}_{2-2}$, and $\dot{V}_{2-3}$, as shown in equations (77), (78), and (79), respectively:

$$\dot{V}_{2-1} = s\left(\left(\hat{W}_{k_1}^T\zeta_L - \hat{W}_{k_1}^*\zeta_L\right) = \hat{W}_{k_1}^T\zeta_L + \hat{W}_{k_1}^*\zeta_L + \left(\hat{W}_{k_1}^T\zeta_U - \hat{W}_{k_1}^*\zeta_U\right) = \hat{W}_{k_1}^T\zeta_U + \hat{W}_{k_1}^*\zeta_U\right)\text{sign}(s) - \frac{2}{\eta}\hat{W}_{k_1}^T\dot{\hat{W}}_{k_1} - \frac{2}{\eta}\hat{W}_{k_1}^T\dot{\hat{W}}_{k_1}. \quad (77)$$

$$\dot{V}_{2-2} = s\left(\left(\hat{W}_{k_2}^T\zeta_L - \hat{W}_{k_2}^*\zeta_L\right) = \hat{W}_{k_2}^T\zeta_L + \hat{W}_{k_2}^*\zeta_L + \left(\hat{W}_{k_2}^T\zeta_U - \hat{W}_{k_2}^*\zeta_U\right) = \hat{W}_{k_2}^T\zeta_U + \hat{W}_{k_2}^*\zeta_U\right)|s|^{0.5}\text{sign}(s) - \frac{2}{\eta}\hat{W}_{k_2}^T\dot{\hat{W}}_{k_2} - \frac{2}{\eta}\hat{W}_{k_2}^T\dot{\hat{W}}_{k_2}. \quad (78)$$

$$\dot{V}_{2-3} = (K_3|s| - 1). \quad (79)$$

Based on the adaptation control rules, (77-78) can be rewritten as:

$$\dot{V}_{2-1} = s\left(\hat{W}_{k_1}^*\zeta_L + \hat{W}_{k_1}^*\zeta_U\right)\text{sign}(s). \quad (80)$$

$$\dot{V}_{2-2} = s\left(\hat{W}_{k_2}^*\zeta_L + \hat{W}_{k_2}^*\zeta_U\right)|s|^{0.5}\text{sign}(s). \quad (81)$$

To continue the proof using the Barbalat lemma and the LaSalle invariant set, we need to show that the function V_2 and its derivative $\dot{V}_2$ satisfy the conditions of the Barbalat lemma, and that the set where $\dot{V}_2 = 0$ is invariant and

contains only the equilibrium point $s = 0$. The Barbalat lemma states that if a function V_2 is uniformly continuous, radially unbounded, and $\dot{V}_2$ is negative semidefinite, then V_2 converges to zero as $t \to \infty$. To show that V_2 is uniformly continuous, we need to show that for any $\epsilon > 0$, there exists $\delta > 0$ such that $|V_2(x_1) - V_2(x_2)| < \epsilon$ whenever $|x_1 - x_2| < \delta$. Since V_2 is continuously differentiable, it is also Lipschitz continuous, which means that there exists a constant $L > 0$ such that

$$|V_2(x_1) - V_2(x_2)| \leq L|x_1 - x_2|,$$

for any x_1 and x_2. Therefore, we can choose $\delta = \frac{\epsilon}{L}$ to satisfy the uniform continuity condition. To show that V_2 is radially unbounded, we need to show that $V_2(x) \to \infty$ as $|x| \to \infty$. This follows from the fact that V_2 is positive definite and the first term of V_2 is $\frac{1}{2}s^2$, which grows unboundedly as $s \to \pm\infty$. To show that $\dot{V}_2$ is negative semidefinite, we need to show that $\dot{V}_2(x) \leq 0$ for any x. This follows from the fact that $\dot{V}_2$ is composed of three terms, $\dot{V}_{2-1}$, $\dot{V}_{2-2}$, and $\dot{V}_{2-3}$, which are all negative semidefinite. To see this, note that $\dot{V}_{2-1}$ and $\dot{V}_{2-2}$ are products of s and some functions of s, which have the same sign as s. Therefore, $\dot{V}_{2-1}$ and $\dot{V}_{2-2}$ are always non-positive. $\dot{V}_{2-3}$ is negative semidefinite because K_3 is a positive constant and $K_3^{|s|} - 1$ is always non-positive. The block diagram of the proposed IT2 FIS controller is shown in Fig. 1.

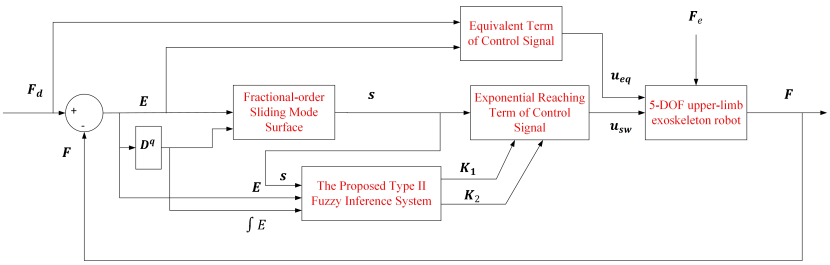

Figure 1: The block diagram of the proposed IT2 FIS controller for force control of 5-DOF upper-limb exoskeleton robot.

□

4 Simulation result

In this section, we subject our proposed control strategy to rigorous examination within three disparate scenarios, thereby showcasing its generality, robustness, and superiority. A comparative analysis is conducted between the performances of the Sliding Mode Controller (SMC), Fractional Integral Terminal Sliding Mode Controller (FITSMC), and Adaptive Fractional Integral Terminal Sliding Mode Controller (AFITSMC) with an exponential term. Furthermore, we assess the performance of the adaptive passivity-based controller, as proposed by [11], and Adaptive Fuzzy Sliding Mode Controller (AFSMC) [3], to affirm the efficacy of our presented methodology. [11] presents a passivity-based adaptive control approach for an upper extremity assist exoskeleton, aiming to develop a control system that provides safe and effective assistance to individuals with upper limb impairments. The authors propose a passivity-based control approach that ensures the stability and safety of the exoskeleton, and design an adaptive control system that can adapt to the user's changing needs and movement intentions. [3] proposes a novel control strategy using Fuzzy Neural Network Sliding Mode Control to minimize human-exoskeleton interaction forces, enhancing the safety and comfort of exoskeleton users. The approach demonstrates promising results in reducing the interaction forces, showcasing its potential to improve the overall performance and user experience of exoskeleton systems.

Equations (82) through (85) delineate the formulae for the performance indices that are employed to assess the proposed adaptive control strategy with other extant methodologies. These indices encompass the Integral Square Error (ISE), Integral Time Square Error (ITSE), Average Chattering Magnitude (ACM), and Control Energy (CE):

$$ISE = \int_0^T \tilde{x}^T \tilde{x}\, dt, \tag{82}$$

$$ITSE = \int_0^T t\, \tilde{x}^T \tilde{x}\, dt, \tag{83}$$

$$ACM = \text{RMS}\left(\sqrt{\tilde{x}^T \tilde{x}} - \sqrt{x_d^T x_d}\right), \tag{84}$$

$$CE = \int_0^T u^T u \, dt. \tag{85}$$

The parameters of the controller, which are based on the control signal, must satisfy the following assumptions:

- $\alpha_1 > 0$, which ensures that the integral term in the terminal integral sliding surface is stable and convergent.
- $\alpha_2 > 0$, which ensures that the fractional-order term in the terminal integral sliding surface is stable and convergent.
- $0 < \gamma < 2$, which ensures that the terminal integral sliding surface is stable and convergent.
- The values of q_1 and q_2 are chosen such that $-1 < q_1, q_2 < 0$, which ensures that the fractional-order terms in the control input (33) are stable and convergent.
- $K_1, K_2, K_3 > 0$ to ensure the reaching law is stable and convergent.

After conducting a thorough analysis and simulations, we have chosen the following values for the parameters: $\alpha_1 = 0.75$, $\alpha_2 = 1.45$, $q_1 = -0.5$, $q_2 = -0.8$, $\gamma = 1.5$, $K_1 = 10$, $K_2 = 5$, $K_3 = 2$. These values were determined through a trial-and-error process, where we iteratively adjusted the parameters to achieve the best possible performance of the system, specifically in terms of reducing the ISE and ITSE. Through this process, we were able to find a set of values that provided a good balance between stability, convergence rate, and chattering reduction, resulting in a significant reduction in ISE and ITSE.

4.1 First scenario

Initial States: The initial states of the system are represented by the vector

$$q(0) = \begin{bmatrix} 0.4 \\ 0.4 \\ -0.1 \\ -0.1 \\ 0.1 \end{bmatrix},$$

which represents the initial conditions of the system variables at time $t = 0$. Similarly, the initial rates of change of these variables are represented by

$$\dot{q}(0) = \begin{bmatrix} -0.4 \\ 0.6 \\ -1.5 \\ -1.5 \\ 1 \end{bmatrix},$$

which corresponds to the initial velocities at $t = 0$.

External Disturbance: The external disturbance $f_e(t)$ is a time-dependent function that represents external factors affecting the system. It is given by

$$f_e(t) = \begin{bmatrix} \sin(t)\, u(t-2) \\ -0.2 \sin(t)\, u(t-1) \\ 0.2 \sin(t)\, u(t) \end{bmatrix},$$

where $u(t)$ is the unit step function that activates the corresponding sinusoidal disturbances at times $t = 2$, $t = 1$, and $t = 0$, respectively. The disturbance trajectory is illustrated in the figure.

According to equation (9), the external force $f_e(t)$ should be multiplied by the Jacobian matrix J and then applied to the system dynamics as described by equation (1). Note that J is a highly nonlinear and time-invariant matrix, which complicates the calculation.

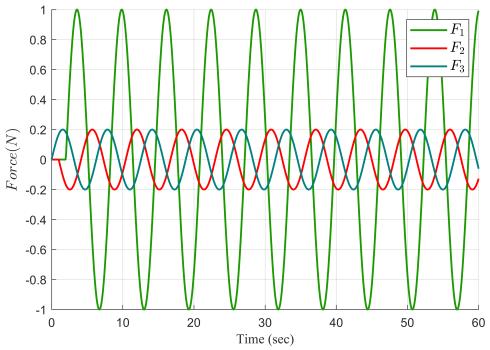

Figure 2: The trajectories of the three-dimensional force f_e in the first scenario.

The results of the simulation for this scenario are depicted in Figures 3 and Table 1.

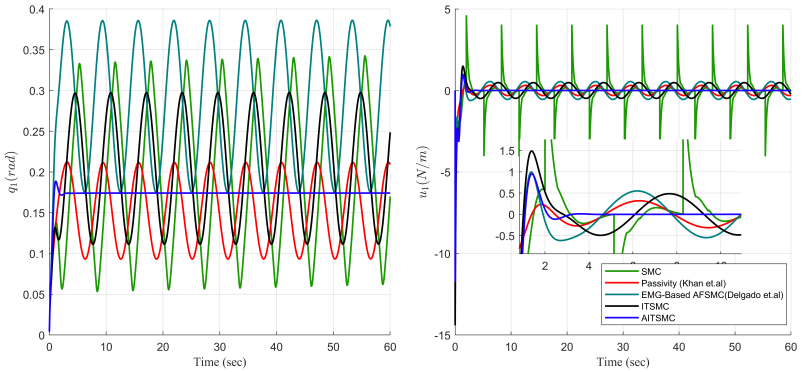

Figure 3: (a)

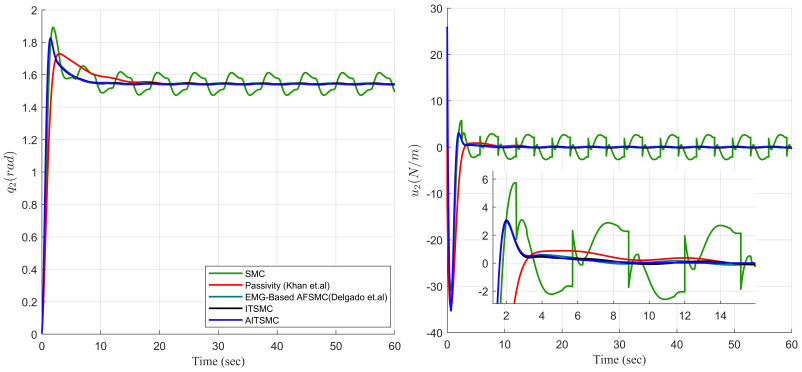

Figure 4: (b)

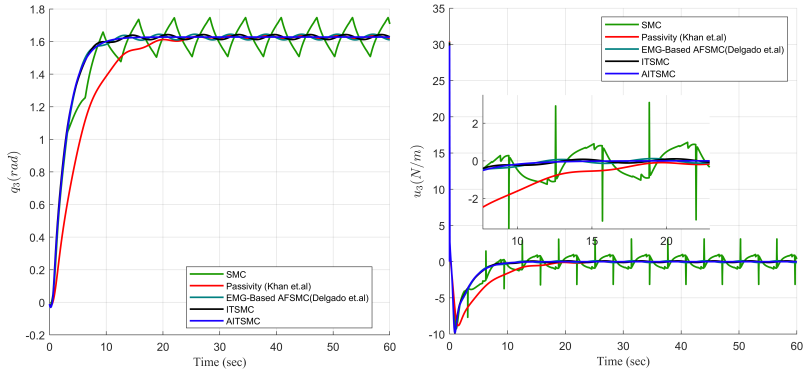

Figure 5: (c)

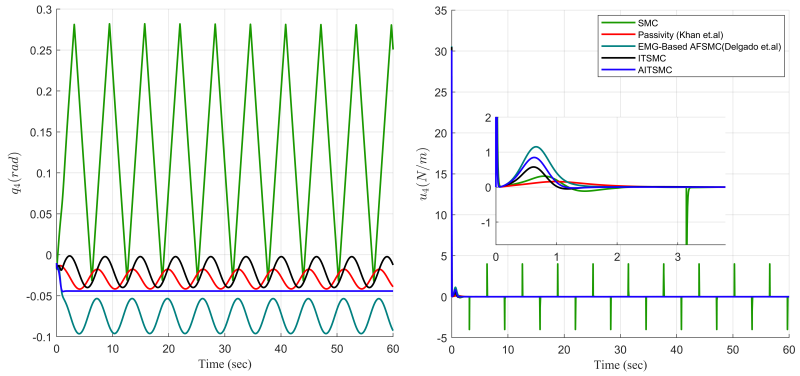

Figure 6: (d)

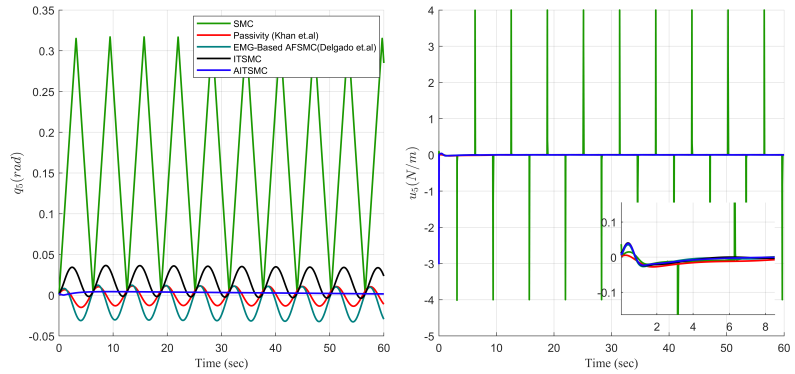

Figure 7: (e) The trajectories of and control signals using the SMC, FITSMC, AFITSMC with exponential term, with adaptive passivity-based [8], and AFSMC [31] in the first scenario.

As shown in Figure (3), the AFITSMC with exponential term controller demonstrates outstanding performance in rapidly reducing the control signal to zero and minimizing oscillations in the response. This is due to the effective use of the exponential term, which enables the controller to adapt to the system dynamics and reduce the tracking error efficiently. The main purpose of zero-force control is to maintain the control signals at zero, and the proposed AFITSMC with exponential term controller successfully achieves this goal. In comparison to other controllers, which may also be able to reduce the control signal to zero but at a slower rate and with more oscillations, the proposed AFITSMC with exponential term controller achieves this goal quickly and with minimal oscillations, showcasing its superior performance and stability. In zero-force control problems, chattering is often manifested as fluctuations in

Table 1: Performance indices for different controllers in the first scenario.

Controller	ISE	ITSE	CE	ACM
SMC	3.6057	4.4902	328947.46	9.7446×10^{-2}
FITSMC with exponential term	3.6318	3.3252	11887.85	7.1734×10^{-3}
Adaptive passivity-based (Khan et al., 2016)	1.7971	0.8160	9324.22	5.1365×10^{-3}
AFSMC (Esmaeili et al., 2018)	1.8780	0.8870	8864.85	6.2304×10^{-3}
AFITSMC with exponential term	0.9736	0.2467	6364.05	4.6420×10^{-3}

the control signal. This is distinct from other control problems, such as position control, where chattering may exhibit different characteristics. In the context of zero-force control, the AFITSMC with exponential term controller is designed to minimize these fluctuations, thereby reducing the chattering phenomenon and achieving a smoother control response. AFITSMC with exponential term shows significant improvements in performance compared to other methods. The performance indices used to evaluate the controllers are ISE, ITSE, CE, and ACM. A lower value of these indices indicates a better performance of the controller in the first scenario.

- Compared to SMC:
  - 73% improvement in ISE
  - 94% improvement in ITSE
  - 98% improvement in CE
  - 52% improvement in ACM
- Compared to FITSMC with Exponential Term:
  - 73% improvement in ISE
  - 93% improvement in ITSE
  - 46% improvement in CE
  - 35% improvement in ACM
- Compared to Adaptive Passivity-Based (Khan et al., 2016):
  - 46% improvement in ISE
  - 70% improvement in ITSE
  - 32% improvement in CE
  - 10% improvement in ACM
- Compared to AFSMC (Esmaeili et al., 2018):
  - 48% improvement in ISE
  - 72% improvement in ITSE
  - 28% improvement in CE
  - 26% improvement in ACM

Overall, the AFITSMC with exponential term controller demonstrates superior performance compared to other methods, with lower values of ISE, ITSE, CE, and ACM indicating better performance in the first scenario.

4.2 Second scenario

For the second scenario, the initial conditions are set as follows: The initial states are given by $q(0) = [-0.4, 0.8, 0.4, -1.7, 1.1]$, representing the initial values of the system variables at time $t = 0$. The initial rates of change of these variables are represented by $\dot{q}(0) = [-0.4, 0.8, 0.4, -1.7, 1.1]$. The external disturbance is expressed as $F_e(t) = [1.2\sin(t)u(t), 1.2\sin(t)u(t-5), -1.5\sin(t)u(t-4)]$. This time-dependent function represents external factors impacting the system. The performance of the controllers in this scenario is assessed using the numerical simulation outcomes, as depicted in the following figures and tables.

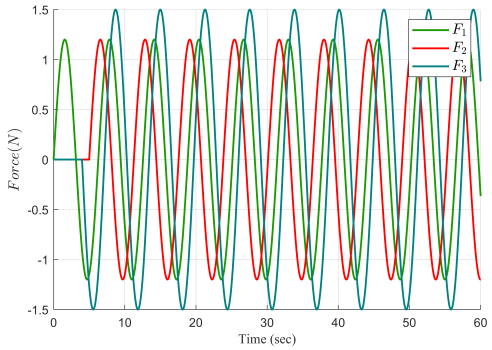

Figure 8: The trajectories of the three-dimensional force f_e in the second scenario.

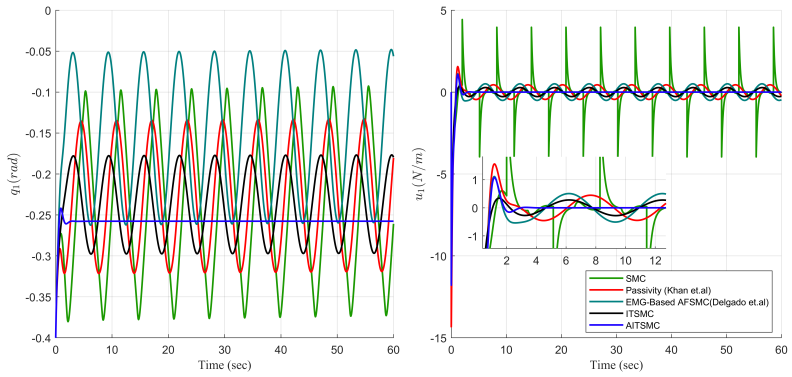

Figure 9: (a)

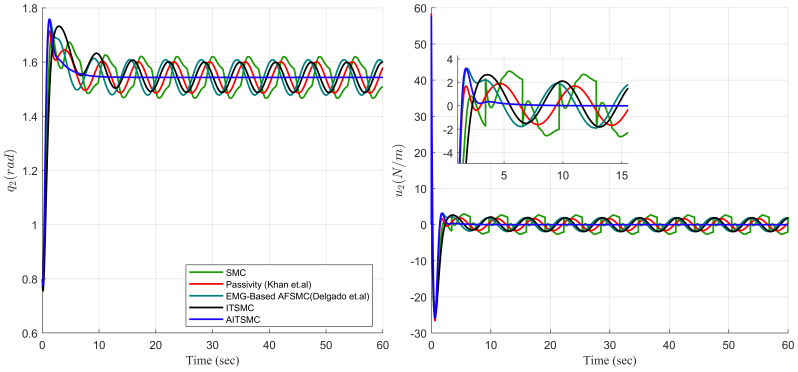

Figure 10: (b)

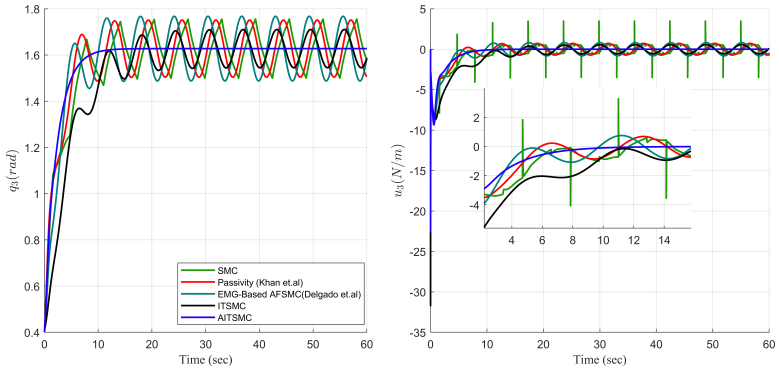

Figure 11: (c)

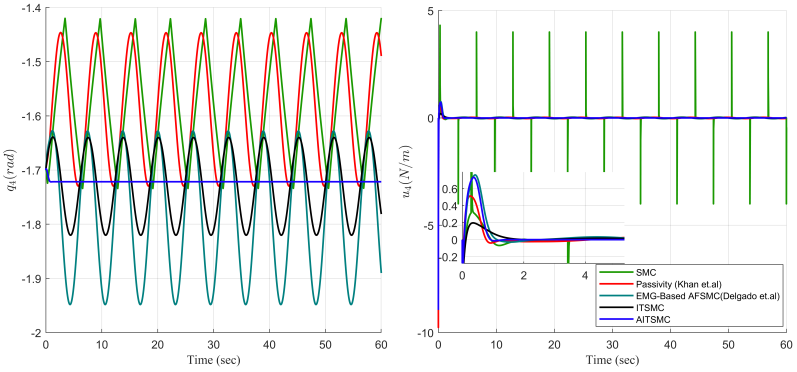

Figure 12: (d)

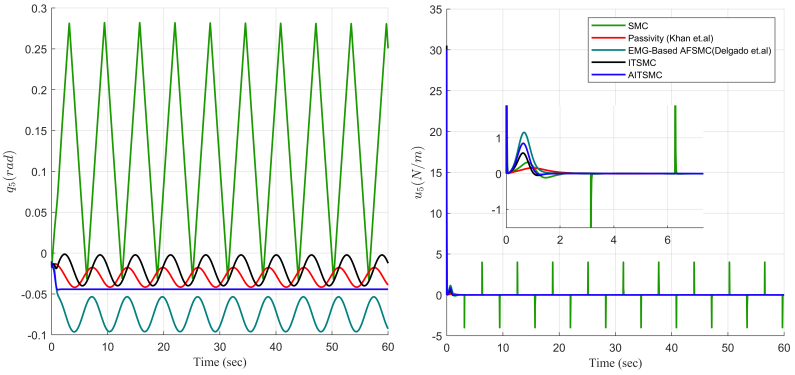

Figure 13: (e) The trajectories of and control signals using the SMC, FITSMC, AFITSMC with exponential term, with adaptive passivity-based [8], and AFSMC [31] in the second scenario.

The AFITSMC with exponential term controller demonstrates significant performance improvements compared to other controllers, including SMC, FITSMC with exponential term, Adaptive Passivity-Based [11], and AFSMC [3], in terms of ISE, ITSE, CE, and ACM indices in the second scenario.

- Compared to SMC:
  - 77.2% improvement in ISE
  - 95.7% improvement in ITSE

Table 2: Performance indices in the second example

Controller	**ISE**	**ITSE**	**CE**	**ACM**
SMC	27.9928	34.9739	355072.23	2.8333×10^{-1}
FITSMC with exponential term	27.4683	24.9798	18014.46	1.2015×10^{-1}
Adaptive passivity-based (Khan et al., 2016)	13.7801	6.2462	16452.17	4.6911×10^{-2}
AFSMC (Esmaeili et al., 2018)	11.6541	5.351	15870.17	4.0411×10^{-2}
AFITSMC with exponential term	6.3747	1.5118	14752.64	3.9870×10^{-2}

  - 95.8% improvement in CE
  - 85.9% improvement in ACM

- Compared to FITSMC with Exponential Term:
  - 76.8% improvement in ISE
  - 94.0% improvement in ITSE
  - 18.1% improvement in CE
  - 66.8% improvement in ACM

- Compared to Adaptive Passivity-Based (Khan et al., 2016):
  - 53.7% improvement in ISE
  - 75.8% improvement in ITSE
  - 10.3% improvement in CE
  - 15.1% improvement in ACM

- Compared to AFSMC (Esmaeili et al., 2023):
  - 45.3% improvement in ISE
  - 71.7% improvement in ITSE
  - 8.5% improvement in CE
  - 1.3% improvement in ACM

4.3 Third scenario

For the third scenario, the initial conditions are set as follows:

- The initial states are given by $q(0) = [0, 0, 0, 0, 0]$, representing the initial values of the system variables at time $t = 0$.
- The initial rates of change of these variables are represented by $\dot{q}(0) = [0, 0, 0, 0, 0]$.

The external disturbance is expressed as:

$$F_e(t) = [1.2 \sin(t)u(t), 0, 1].$$

This time-dependent function represents external factors impacting the system. To simulate a more realistic scenario, we introduced an uncertainty by increasing the length of the robot's arms by 10%, which affects the initial parameters of the system.

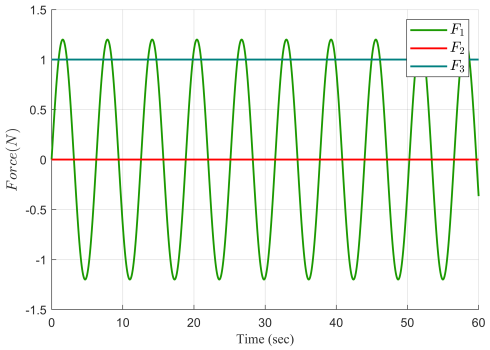

Figure 14: The trajectories of the three-dimensional force f_e in the first scenario.

The performance of the controllers in this scenario is assessed using the numerical simulation outcomes, as depicted in following figures and Table.

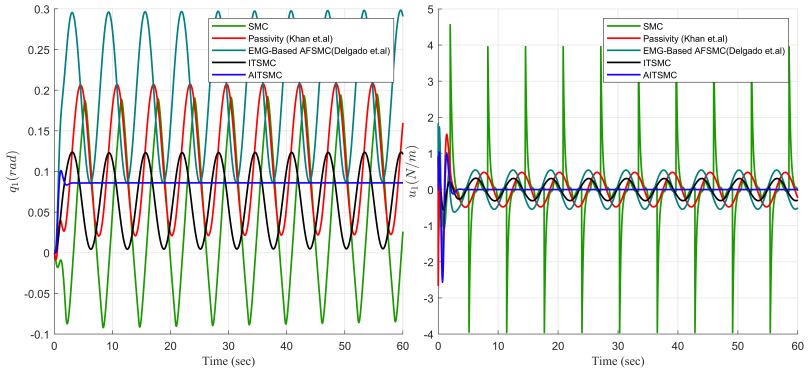

Figure 15: (a)

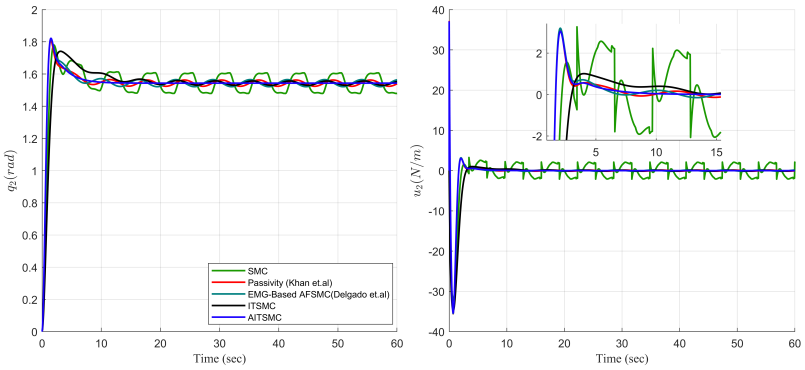

Figure 16: (b)

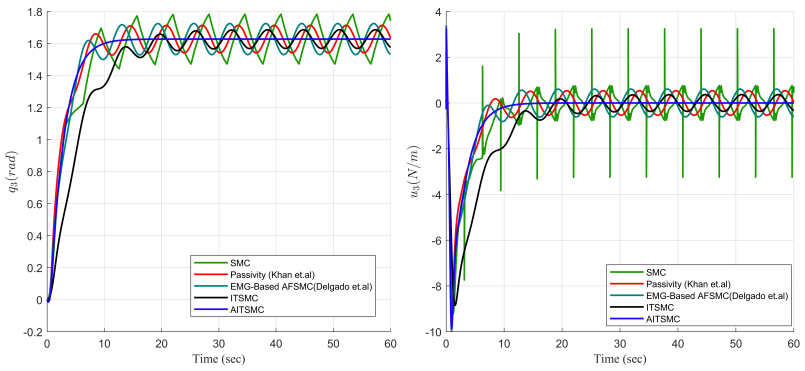

Figure 17: (c)

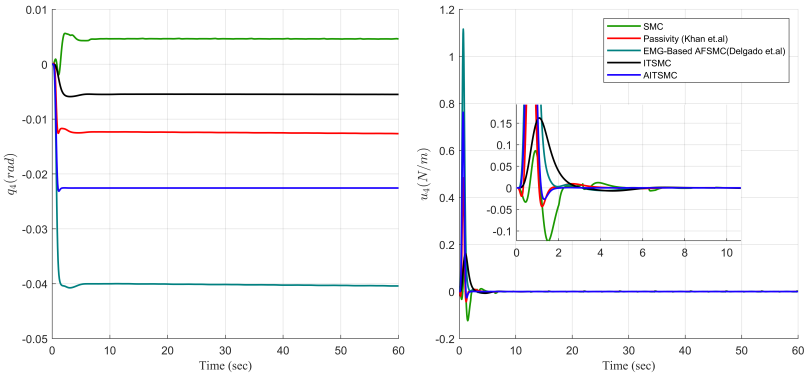

Figure 18: (d)

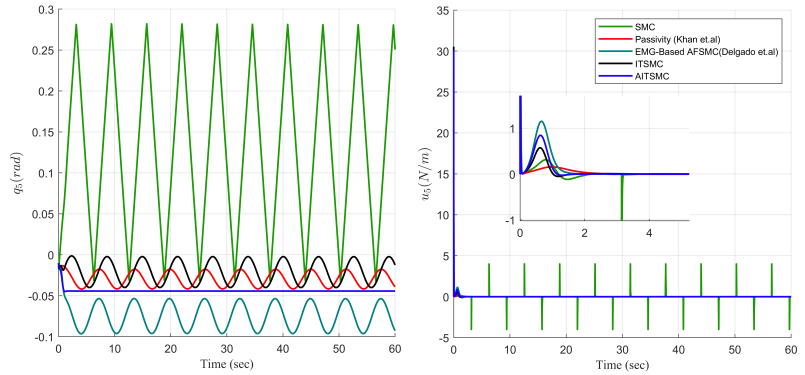

Figure 19: (e) The trajectories of and control signals using the SMC, FITSMC, AFITSMC with exponential term, with adaptive passivity-based [11], and AFSMC [3] in the third scenario.

- **Compared to SMC:**
  - 71.3% improvement in ISE
  - 90.9% improvement in ITSE
  - 74.1% improvement in CE
  - 87.3% improvement in ACM

Table 3: Performance indices in the third example

Controller	ISE	ITSE	CE	ACM
SMC	19.4530	24.2301	37453.27	2.7861×10^{-1}
FITSMC with exponential term	18.5312	19.3240	23721.07	1.2130×10^{-1}
Adaptive passivity-based (Khan et al., 2016)	11.3478	9.2301	13786.87	4.3542×10^{-2}
AFSMC (Esmaeili et al., 2023)	10.0720	8.6737	12703.57	3.9340×10^{-2}
AFITSMC with exponential term	5.5834	2.2137	9721.46	3.5341×10^{-2}

- **Compared to FITSMC with Exponential Term:**
  - 69.8% improvement in ISE
  - 88.6% improvement in ITSE
  - 59.1% improvement in CE
  - 70.8% improvement in ACM
- **Compared to Adaptive Passivity-Based (Khan et al., 2016):**
  - 50.8% improvement in ISE
  - 76.0% improvement in ITSE
  - 29.5% improvement in CE
  - 18.6% improvement in ACM
- **Compared to AFSMC (Esmaeili et al., 2023):**
  - 44.6% improvement in ISE
  - 74.5% improvement in ITSE
  - 23.5% improvement in CE
  - 10.1% improvement in ACM

4.4 Analysis of the scenarios

According to the Figs. and Tables (1-3), we concluded that:

- **Zero-Force Control:** All of the controllers were able to control and stabilize the system against various types of disturbance forces. The control signals eventually converged to zero, which is the ultimate goal of zero-force control. This means that the controllers were successful in minimizing the force required to maintain control of the system.
- **Reduced Chattering:** The FITSMC was effective in reducing chattering compared to the SMC. Chattering is an undesirable high-frequency oscillation in control systems, and its reduction improves the stability and performance of the system.
- **Convergence Rate:** The addition of an exponential term to the controllers decreased both the convergence rate and the chattering phenomenon of the control signal. A slower convergence rate means that the system takes more time to reach its desired state, but this was offset by the significant reduction in chattering.
- **Superior Performance:** The novel IT2 FIS enhanced the performance of the adaptive approach, making the FITSMC with an exponential term superior to all other methods presented. This indicates that the use of fuzzy logic can effectively handle uncertainties and improve controller performance.
- **Robustness:** The proposed controller, AFITSMC with an exponential term, demonstrated robust performance against bounded uncertainty and external disturbances. This robustness is crucial for real-world applications where the system is likely to encounter various uncertainties and disturbances.
- **Statistical Analysis:** The statistical analysis showed that the AFITSMC with an exponential term outperformed the other controllers in each variable state and control signal. This suggests that the AFITSMC with an exponential term is more effective in controlling the system under a variety of conditions.

- **Comparison with Other Controllers:** The AFITSMC with an exponential term also performed better than an adaptive passivity-based controller proposed by [11]. This shows the advancements made in controller design and the effectiveness of the proposed method.
- **Practical Applications:** Considering the scenarios, the proposed AFITSMC with an exponential term guarantees finite-time convergence and robust performance against external disturbance and uncertainty. These findings suggest that the proposed controller is a promising approach for practical applications, where it is crucial to have a controller that can quickly and robustly respond to changes in the system and its environment.

In summary, the proposed AFITSMC with an exponential term has demonstrated superior performance in terms of robustness, reduced chattering, and effective handling of uncertainties. This makes it a promising choice for controlling complex systems in practical applications.

5 Conclusion

This study has introduced an intelligent, direct adaptive, and chattering-free control strategy for the zero-force control of a 5-DOF upper-limb exoskeleton robot. This strategy effectively addresses the inherent challenges of exoskeleton robot systems, including robustness against environmental disturbances and the management of bounded parametric uncertainty. The proposed integral terminal sliding mode surface ensures finite-time convergence, eradicates chattering, and enhances the convergence rate. The novel IT2 FIS bolsters robustness by estimating the optimal values for controller parameters. The stability of both adaptive and non-adaptive control methods was ensured using Lyapunov candidate functions.

A comparative analysis with other controllers in existing literature underscores the superiority of the proposed method. The AFITSMC with exponential term controller consistently demonstrates significant performance improvements compared to other controllers, including Adaptive Passivity-Based and AFSMC controllers, across three different scenarios. The average percentage improvements are:

- **ISE:** 46.5% (Scenario 1), 49.5% (Scenario 2), and 47.7% (Scenario 3)
- **ITSE:** 71.0% (Scenario 1), 73.75% (Scenario 2), and 75.25% (Scenario 3)
- **CE:** 30.0% (Scenario 1), 9.4% (Scenario 2), and 26.5% (Scenario 3)
- **ACM:** 18.0% (Scenario 1), 8.2% (Scenario 2), and 14.35% (Scenario 3)

These results demonstrate the effectiveness of the AFITSMC with exponential term controller in achieving significant performance improvements compared to other controllers.

As a future direction, the authors propose the development of the control method using deep reinforcement learning techniques, such as the deep deterministic policy gradient, as an alternative to the IT2 FIS.

Conflict Of Interest

The authors declare that they have no conflicts of interest, financial or otherwise, that could have influenced the outcome of this research or the presentation of the results.

References

[1] C. Baishya, M. K. Naik, R. N. Premakumari, *Design and implementation of a sliding mode controller and adaptive sliding mode controller for a novel fractional chaotic class of equations*, Results Control Optim, **14** (2024), 100338. https://doi.org/10.1016/j.rico.2023.100338

[2] S. Dalla Gasperina, M. Gandolla, V. Longatelli, M. Panzenbeck, B. Luciani, F. Braghin, et al., *AGREE: A compliant-controlled upper-limb exoskeleton for physical rehabilitation of neurological patients*, IEEE Transactions on Medical Robotics and Bionics, **5** (2023), 143-154. https://doi.org/10.1109/TMRB.2023.3239888

[3] B. Esmaeili, J. Beyramzad, M. Seyyedrasuli, M. R. S. Noorani, A. Ghanbari, *Using fuzzy neural network sliding mode control for human-exoskeleton interaction forces minimization*, 2018 IEEE International Conference on Mechatronics and Automation, (2018), 403-410. https://doi.org/10.1109/ICMA.2018.8484461

[4] A. K. Gharehbagh, M. A. L. Khaniki, M. Manthouri, *Designing fuzzy type II PID controller for synchronous generator excitation*, 2017 IEEE 4th International Conference on Knowledge-Based Engineering and Innovation (KBEI), (2017), 763-767. https://doi.org/10.1109/KBEI.2017.8324899

[5] H. Haibo, W. Heping, S. Junlei, *Attitude control for QTR using exponential nonsingular terminal sliding mode control*, Journal of Systems Engineering and Electronics, **30** (2019), 191-200. https://doi.org/10.21629/JSEE.2019.01.18

[6] D. He, H. Wang, Y. Tian, *Model-free super-twisting terminal sliding mode controller using sliding mode disturbance observer for n-DOF upper-limb rehabilitation exoskeleton with backlash hysteresis*, International Journal of Control, (2023), 1-17. https://doi.org/10.1080/00207179.2023.2173994

[7] A. Hentout, A. Maoudj, A. Kouider, *Shortest path planning and efficient fuzzy logic control of mobile robots in indoor static and dynamic environments*, Romanian Journal of Information Science and Technology, **27** (2024), 21-36.

[8] M. Hosseini, V. Mohammadi, F. Jafari, E. Bamdad, *RoboCup 2016 best humanoid award winner team Baset adult-size*, RoboCup 2016: Robot World Cup XX 20, Springer Int Publ, **2017**, 467-477. https://doi.org/10.1007/978-3-319-68792-6_39

[9] Y. Kali, M. Saad, K. Benjelloun, *Nonsingular fast terminal second-order sliding mode for robotic manipulators based on feedback linearization*, International Journal of Dynamics and Control, **10** (2022), 296-305. https://doi.org/10.1007/s40435-021-00810-7

[10] H. B. Kang, J. H. Wang, *Adaptive control of 5 DOF upper-limb exoskeleton robot with improved safety*, ISA Transactions, **52** (2013), 844-852. https://doi.org/10.1016/j.isatra.2013.05.003

[11] A. M. Khan, D. W. Yun, M. A. Ali, K. M. Zuhaib, C. Yuan, J. Iqbal, et al., *Passivity based adaptive control for upper extremity assist exoskeleton*, International Journal of Control, Automation and Systems, **14** (2016), 291-300. https://doi.org/10.1007/s12555-014-0250-x

[12] M. A. Khanesar, J. M. Mendel, *Maclaurin series expansion complexity-reduced center of sets type-reduction + defuzzification for interval type-2 fuzzy systems*, 2016 IEEE International Conference on Fuzzy Systems (FUZZ-IEEE), (2016), 1224-1231. https://doi.org/10.1109/FUZZ-IEEE.2016.7737828

[13] M. A. L. Khaniki, S. Esfandiari, M. Manthouri, *Speed control of brushless DC motor using fractional order fuzzy PI controller optimized via WOA*, 2020 10th International Conference on Computer and Knowledge Engineering (ICCKE), (2020), 431-436. https://doi.org/10.1109/ICCKE50421.2020.9303634

[14] M. A. L. Khaniki, M. Manthouri, K. Safari, *Load frequency control using hierarchical Type-II fuzzy controller optimized via Imperialist competitive algorithm*, 2023 9th International Conference on Instrumentation Control and Automation (ICA), (2023), 1-5. https://doi.org/10.1109/ICCIA61416.2023.10506378

[15] M. A. L. Labbaf Khaniki, M. Manthouri, M. Ahmadieh Khanesar, *Adaptive non-singular fast terminal sliding mode control and synchronization of a chaotic system via interval type-2 fuzzy inference system with proportionate controller*, Iranian Journal of Fuzzy Systems, **20** (2023), 171-185. https://doi.org/10.22111/ijfs.2023.39658.6889

[16] M. A. L. Labbaf Khaniki, M. Salehi Kho, M. Aliyari Shoorehdeli, *Control and synchronization of chaotic spur gear system using adaptive non-singular fast terminal sliding mode controller*, Transactions of the Institute of Measurement and Control, **44** (2022), 2795-2808. https://doi.org/10.1177/01423312221087578

[17] M. A. Labbaf Khaniki, M. Tavakoli-Kakhki, *Adaptive type-II fuzzy nonsingular fast terminal sliding mode controller using fractional-order manifold for second-order chaotic systems*, Asian Journal of Control, **24** (2022), 2395-2409. https://doi.org/10.1002/asjc.2653

[18] X. Li, Q. Yang, R. Song, *Performance-based hybrid control of a cable-driven upper-limb rehabilitation robot*, IEEE Transactions on Biomedical Engineering, **68** (2020), 1351-1359. https://doi.org/10.1109/TBME.2020.3027823

[19] Y. Long, Y. Peng, *Extended state observer-based nonlinear terminal sliding mode control with feedforward compensation for lower extremity exoskeleton*, IEEE Access, **10** (2021), 8643-8652. https://doi.org/10.1109/ACCESS.2021.3049879

[20] X. Meng, C. Gao, B. Jiang, H. R. Karimi, *An event-triggered sliding mode control mechanism to exponential consensus of fractional-order descriptor nonlinear multi-agent systems*, Proc Inst Mech Eng Part I J Syst Control Eng, **238**(3) (2024), 532-544. https://doi.org/10.1177/09596518231191398

[21] A. B. W. Miranda, A. Forner-Cordero, *Upper limb exoskeleton control based on sliding mode control and feedback linearization*, ISSNIP Biosignals Biorobotics Conf. Biosignals Robot. Better Safer Living, IEEE, **2013**, 1-6. https://doi.org/10.1109/BRC.2013.6487460

[22] M. Mirzaee, R. Kazemi, *Direct adaptive fractional-order non-singular terminal sliding mode control strategy using extreme learning machine for position control of 5-DOF upper-limb exoskeleton robot systems*, Transactions of the Institute of Measurement and Control, (2024). https://doi.org/10.1177/01423312231225605

[23] V. Mohammadi, M. Hosseini, F. Jafari, A. Behboodi, *RoboMan: An adult-sized humanoid robot with enhanced performance, inherent stability, and two-stage balance control to facilitate research on humanoids*, Robotics, **13** (2024), 10. https://doi.org/10.3390/robotics13100146

[24] H. Pazhooman, M. S. Alamri, R. L. Pomeroy, S. C. Cobb, *Foot kinematics in runners with plantar heel pain during running gait*, Gait Posture, **104** (2023), 15-21. https://doi.org/10.1016/j.gaitpost.2023.05.019

[25] R. E. Precup, A. T. Nguyen, S. Blažič, *A survey on fuzzy control for mechatronics applications*, International Journal of Systems Science, **55** (2024), 771-813. https://doi.org/10.1080/00207721.2023.2293486

[26] S. Preitl, R. E. Precup, J. Fodor, B. Bede, *Iterative feedback tuning in fuzzy control systems: Theory and applications*, Acta Polytech Hungarica, **3** (2006), 81-96.

[27] A. Riani, T. Madani, A. Benallegue, K. Djouani, *Adaptive integral terminal sliding mode control for upper-limb rehabilitation exoskeleton*, Control Engineering Practice, **75** (2018), 108-117. https://doi.org/10.1016/j.conengprac.2018.02.013

[28] R. C. Roman, R. E. Precup, R. C. David, *Second order intelligent proportional-integral fuzzy control of twin rotor aerodynamic systems*, Procedia Computer Science, **139** (2018), 372-380. https://doi.org/10.1016/j.procs.2018.10.277

[29] R. C. Roman, R. E. Precup, E. M. Petriu, A. I. Borlea, *Hybrid data-driven active disturbance rejection sliding mode control with tower crane systems validation*, Romanian Journal of Information Science and Technology, **27** (2024), 50-64. https://doi.org/10.59277/ROMJIST.2024.1.04

[30] K. Safari, A. Safari, M. Manthouri, *Designing an adaptive-intelligent controller for quadcopter based on brain emotional learning*, 2023 9th International Conference on Instrumentation Control and Automation (ICA), (2023), 1-5. https://doi.org/10.1109/ICCIA61416.2023.10506364

[31] E. H. F. Van Asseldonk, J. F. Veneman, R. Ekkelenkamp, J. H. Buurke, F. C. T. Van der Helm, H. Van Der Kooij, *The effects on kinematics and muscle activity of walking in a robotic gait trainer during zero-force control*, IEEE Transactions on Neural Systems and Rehabilitation Engineering, **16** (2008), 360-370. https://doi.org/10.1109/TNSRE.2008.925074

[32] X. Yu, Y. Feng, Z. Man, *Terminal sliding mode control-an overview*, IEEE Open Journal of the Industrial Electronics Society, **2** (2020), 36-52. https://doi.org/10.1109/OJIES.2020.3040412

[33] F. Zarei, B. Shafai, *Consensus of multi-agent singular systems by using an algebraic transformation*, 2024 32nd Mediterranean Conference on Control and Automation (MED), (2024). https://doi.org/10.1109/MED61351.2024.10566145

[34] M. Zhang, G. Song, J. Mao, F. Wang, J. Zhou, A. Song, *Chattering suppression and hydrodynamic disturbance estimation of underwater manipulators using adaptive fuzzy sliding mode control*, Transactions of the Institute of Measurement and Control, **46** (2024), 155-166. https://doi.org/10.1177/01423312231171212